A continuous parameter-based approach to model the effect of mechanical stress on the electromagnetic hysteresis characteristic

Benedikt Schauerte, Simon Steentjes, Nora Leuning and Kay Hameyer

Institute of Electrical Machines (IEM), RWTH Aachen University, D-52062 Aachen, Germany

Increasing rotating frequencies of electrical machines to maximize the power density lead to higher tensile and compressive mechanical stresses that are distributed inhomogeneously along the rotors' cross section and add up to the already present residual stresses induced by the preceding manufacturing and processing steps. These effects are either neglected or considered only in the post-processing of the machine layout and design.Neglecting the mechanical impact on the magnetic properties during numerical machine simulations leads to uncertainties and deviations from the actual material behavior. This deviations are transmitted to the subsequent loss calculation and further post-processing resulting in inaccurate loss maps. In this paper the influence of mechanical stress on the hysteresis properties and occurring losses of a non-oriented soft magnetic material are examined and replicated by an adjusted energy-based hysteresis model. The chosen models ability to recreate the observed behavior for both, anhysteretic and hysteretic components, will then be evaluated. The evaluation of the model will be performed with focus on a variety of characteristic magnetic properties. Namely the required maximum magnetic field, measured and simulated losses and the ability of the model, to recreate the actual measured magnetic flux paths including the remanence polarisation and coercive magnetic field.

***Index Terms*—hysteresis modeling, non-oriented electrical steel, mechanical stress**

I. Introduction

Magnetic properties of soft magnetic steel sheets alter significantly mainly due to mechanical stress [1]. This mechanical stress originates either from the different manufacturing processes [2]–[4] or the operation of electrical machines, e.g., centrifugal force or magnetic forces [5]. A large variety of publications deals with the influence of mechanical stress on the losses with respect to the magnetic flux density B and the applied frequency f and the modelling of these effects [6]–[8]. Despite this high interest in this topic, only few authors dealt with the consideration of mechanical stresses and their influence on the static hysteresis pathways and the modeling of this effects [9]. The static hysteresis models that are used in the design process to represent the constitutive relation between the magnetic flux density and magnetic field are parametrized usually by means of standardized magnetic measurements on a single-sheet tester (SST) or Epstein frame according to the IEC 60404-2 and IEC 60404-3 standards. During these measurements either stress-relief annealed samples or samples that are made by a gentle method of cutting, e.g., wire or water jet cutting, are used. Commonly, the samples are not subjected to any external mechanical stress or specific residual stress during the measurements. However, when measuring the hysteresis loops of samples that are processed by a specific non-gentle method of cutting, such as blanking or laser cutting, samples of different width or assembled magnetic components, various hysteresis loop shapes can be obtained. These can deviate significantly from the hysteresis loop shapes of unprocessed (or gently-processed) soft magnetic material.

Neglecting stress effects leads to a strong simplification that is often inadequate when considering the influence of the varying magnetic properties on the simulated hysteresis loop shape and its dynamic behavior. This paper presents a thorough analysis of the effects of internal mechanical stress state on the static hysteresis loop and an efficient approach to include the magneto-elastic coupling in an energy-based hysteresis model. A study of the influence of mechanical loads on the magnetic material properties and their consideration by an energy-based hysteresis model enables a more accurate design and simulation of the machine behavior.

This energy-based hysteresis model is based on the decomposition of total field strength into reversible and irreversible components and yields a continuous description of the magnetic field H calculated by analytical formulations based in a set of eight parameters. The model allows the continuous description of the resulting H-curves for arbitrary inputs of B like minor loops and is adjusted for the usage in FEM-machine calculations. For an improved accuracy of the simulation results, the reversible anhysteretic components are recreated by an adjusted formulation, differing from their classical representations.

The values of the model parameters are determined by using experimental data, obtained at an uniaxial SST, which is equipped with a tensile and compression hydraulic loading unit. This enables the application of uniaxial mechanical stress collinear to the magnetic flux up to a maximum force of $5\,\mathrm{kN}$.

II. Measurements

The measurements were performed with a commercially available, non-oriented soft magnetic material with a silicon content of 2.4% and a thickness of 0.5 mm. An overview of all the chemical components is given in Tab. I. The specimens with a measured conductivity of $0.386\,\Omega\mathrm{mm}^2/\mathrm{m}$ were cut into sheets of 600 mm length and a width of 100 mm. The utilized one-dimensional SST allows the characterization of magnetic properties under the influence of tensile and compressive uniaxial mechanical loads collinear to the magnetic flux in the elastic range of the material.

978-1-5386-6425-4/18/$31.00 ©2018 IEEE

TABLE I: Chemical composition of examined non-oriented electrical steel.

Element	Fe	C	Si	Mn	P	S	Cr	Al
wt %	97	0.02	2.42	0.16	0.02	0.01	0.03	0.34

The SST is incorporated into a computer-aided setup according to the international standard IEC 604043 and the magnetic flux is controlled to be sinusoidal in time with the averaged deviation from the predefined sinusoidal signal as the controlled variable [10].
The magnetic characterization is performed by the application of controlled excitation currents in order to obtain sinusoidal magnetic flux densities at a frequency of 50 Hz. By removing the classical eddy current field components H_{cl} qualitative representations $H_{\mathrm{rep,dc}}$ of static hysteresis curves can be obtained following (1) for the known material conductivity σ and sheet thickness d [13]. This allows an approximate estimate of the static curves to be made, although some error liability, such as the neglect of the excess field components, must be taken into account. Nonetheless, this estimation allows the investigation of the suitability of the model to map the magnetomechanical dependencies.

$$H_{\mathrm{rep,dc}} = H_{50\mathrm{Hz}} - \frac{\sigma \pi d^2}{12} \frac{\mathrm{d}B}{\mathrm{d}t} \tag{1}$$

The resulting losses can be calculated by integrations of the hysteresis curves reduced by these magnetic field components. Fig. 1 depicts the resulting quasi-static hysteresis curves at different stress levels, revealing the strong dependency between the characteristic magnetic properties and the applied mechanical stress.

Next to decreased permeabilities over the entire range of magnetic flux density at each controlled value of maximum excitation B_{m} deterioration of the general magnetic behavior in terms of the typical desired soft magnetic characteristics - like a low coercive field H_{c} and a high remanence B_{r} can be denoted as depicted in Fig. 2. These characteristic values are a good measure for the soft-magnetic quality of non oriented materials, as a low coercive field combined with a high remanence polarization reveals low hysteresis losses as also high permeabilities.

While the coercive field H_{cl} decreases for small tensile stresses, the global behavior shows a clear negative trend with increasing coercive field strengths and reduced remanence polarizations for both, tensile and compressive stresses. The magnetic properties generally react more sensitive to compressive stress. Despite the similar deterioration for both stress orientations, the influence of mechanical stress on the respective hysteresis loop shapes differs. While the hysteresis curve for the unloaded case is rather rectangular, in particular for high excitations to high saturation, a mechanical loading in both directions leads to a more S-shaped form and a shearing of the obtained curves. Particularly for tensile stress, where mechanically conditioned, a wider range of loads can be applied, both characteristic values show a distinctive relation to the applied mechanical stress. For the coercive field H_{c},

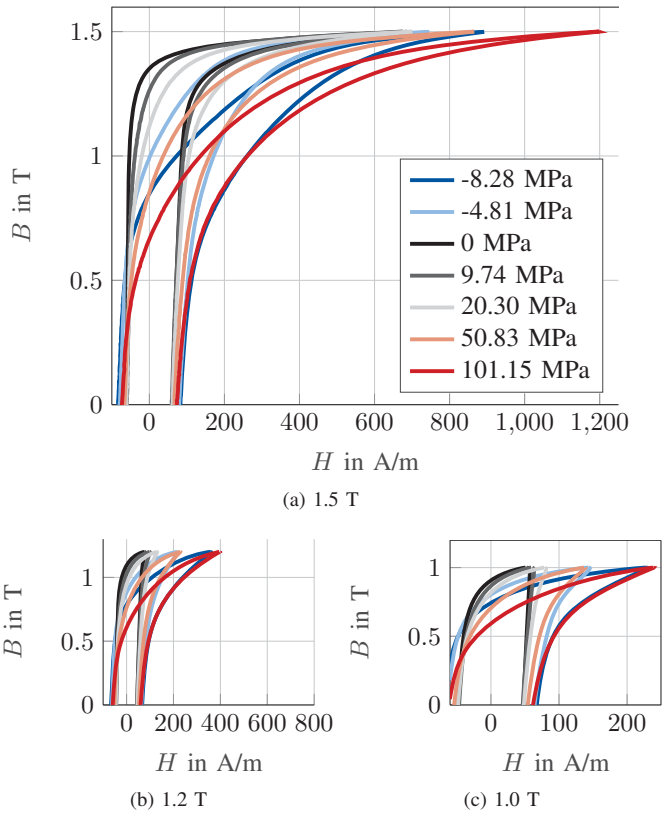

Fig. 1: Measured hysteresis curves for different mechanic stresses at different saturations.

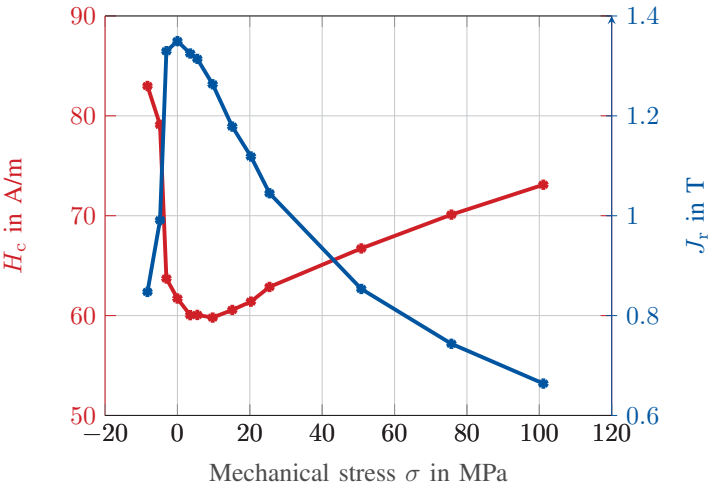

Fig. 2: Measured coercive field H_{c} and remanence polarization J_{r} at 1.5 T as a function of the applied mechanical stress.

a linear increasing relationship to the tensile mechanical load can be observed, while the remanence polarization appears to decrease in an exponential slope.

III. Hysteresis Modelling

For the reproduction of the measured magnetic behavior with respect to the applied mechanical stress an energy-based hysteresis model introduced in [11] and [12] is used as a

groundwork and extended. The hysteresis model uses the magnetic flux density B as the independent field variable. The magnetic field H is separated into an anhysteretic component H_{An}, and a hysteretic component H_{H}, that considers the energy loss linked to the jerky domain-wall motion. In contrast to the original model [11], this paper utilizes a set of two Langevin functions $\mathcal{L}$ to represent the anhysteretic field H_{An} as introduced in [14]:

$$B = \mu_0(H + M_{\mathrm{S}}(w\mathcal{L}(\frac{H+\alpha_{\mathrm{a}}M}{a}) + (1-w)\mathcal{L}(\frac{H+\alpha_{\mathrm{b}}M}{b})) \tag{2}$$

with

$$\mathcal{L}(x) = \coth(x) - \frac{1}{x} \tag{3}$$

Both parameters $\alpha_{\mathrm{a,b}}$ lead to a shearing of the resulting anhysteretic curve and represent the coupling between the magnetic domains moments and their magnetization state within the material as proposed in the original version of the JA-model [15]. The two parameters a and b determine the slope of the two curves in a nonlinear, anti-proportional fashion. The first function $\mathcal{L}(a, \alpha_{\mathrm{a}})$ represents the strong slope of the magnetization curves in the unsaturated state at low values of the applied magnetic field H. The purpose of the additional second function $\mathcal{L}(b, \alpha_{\mathrm{b}})$ is the recreation of the vectorial turning processes within the magnetic domains in the regions of higher excitation. As the saturation magnetization M_{S} is no arbitrary model parameter and each Langevin function strives against a final value of one, the two functions are normalized to a cumulative value of one. This normalization is performed by means of the weighting parameter w which considerably influences the pathway of the obtained anhysteretic magnetization curve.

In general, the double Langevin function approach allows the recreation of more sophisticated curve pathways and is more versatile in terms of the established slopes than the single function approach. As the utilized model calculates the magnetic field as a function of a given pathway of the magnetic flux density, the description of the anhysteretic magnetization has to be inverted. This inversion is given by means of:

$$H_{\mathrm{An}} = \frac{B}{\mu_0} - M_{\mathrm{S}}[w\,\mathcal{L}(\lambda_{\mathrm{a}}) + (1-w)\mathcal{L}(\lambda_{\mathrm{b}})] \tag{4}$$

with the input parameters:

$$\lambda_{\mathrm{a,b}} = \frac{H_{\mathrm{An}}(1-\alpha_{\mathrm{a,b}}) + B(\frac{\alpha_{\mathrm{a,b}}}{\mu_0})}{a_{\mathrm{a,b}}} \tag{5}$$

.

The additional hysteretic field-component H_{H} represents the additional amount of energy that has to be applied due to the loss-connected domain wall movements and determines the resulting slopes of the obtained hysteresis curves as the occurring losses. Its differential relation with the applied magnetic flux density can be expressed as:

$$\frac{\mathrm{d}H_{\mathrm{H}}}{\mathrm{d}B} = \frac{H_{\mathrm{HS}}\mathcal{L}(\lambda)_{\mathrm{H}} - H_{\mathrm{H}}}{I_{\mathrm{D}}\gamma_{\mathrm{H}}} \tag{6}$$

.

For interative calculations the expression (6) is rewritten to the following expression which yields the irreversible field component H_{H} by the numerical solution of:

$$I_{\mathrm{D}}\gamma_{\mathrm{H}}(H_{\mathrm{H}} - H_{\mathrm{H,0}}) = (B_{\mathrm{H}} - B_{\mathrm{B,0}})(H_{\mathrm{HS}}\mathcal{L}(\lambda_{\mathrm{H}}) - H_{\mathrm{H}}) \tag{7}$$

.

Again, a Langevin function is utilized, this time with the input λ_{H} in order to describe behavior of the irreversible field component with respect to the magnetic flux density B:

$$\lambda_{\mathrm{H}} = \frac{H_{\mathrm{H}} + I_{\mathrm{D}}H_{\mathrm{HS}}}{a_{\mathrm{H}}} \tag{8}$$

I_{D} denotes the sign of the magnetic-flux-density change from the value at the previous step B_0 to the current step B. The model Parameter γ_{H} increases the width of the hysteresis loop as the initial slope of the hysteretic field component H_{H} initally after the turning point [12]. The total width of the hysteresis loop and with it the hysteresis losses are also controlled by the model Parameter H_{HS} which describes the maximum value of the irreversible magnetic field. H_{H0} denotes the previous value of H_{H}, B_{B0} is the applied magnetic flux density in the previous calculation step.
The sought-after H_{H} occurs on both sides of the equation and is also an input for the langevin function.

Thus it can not be calculated directly. H_{H} has to be determined by iterative algorithms, such as Newtons method. The input variable for the Langevin function λ_{H} can be calculated by means of H_{HS} and model parameter a_{H}. A thorough analysis on the parameter sensitivity of the model is presented in [16]. In order to recreate the obtained hysteresis loop shapes at different mechanical loads, the model parameters are identified by means of a mathematical error minimization scheme on base of the Levenberg-Marquardt algorithm for each applied mechanical load. The resulting simulated curves will be presented and discussed in the following section.

For each measured hysteresis curve excited to 1.5 T a set of eight parameters was identified by numerical absolute error-reduction methods. The resulting simulated curves and their corresponding measurements are depicted in Fig. 3 and reveal an acceptable agreement across the entire range of applied mechanical loads for high magnetic flux densities. Particularly in the range of no and small tensile stress where the shearing of the hysteresis curves is small, the agreement between measurement and simulation is very satisfactory for the hyseresis curves measured at 1.5 T. At lower excitations the agreement between simulations and measurements deteriorates increasingly.

For higher mechanical loads the shape of the magnetization curves differs more and more from the typical form of non-oriented magnetization curves with a high slope around low

excitation fields and early saturation reached at low magnetic fields and high polarizations. The transition from high permeabilities to saturation is now distributed smoother over the entire saturation range. Thus, the model faces difficulties at the recreation of these loop shapes as the magnetization behavior diverges more and more from the typical observed curves. These measured curves for high mechanical loads differ strongly from the unloaded curves that can be recreated by classical parametric hysteresis models with good agreement. Nonetheless, the double-Langevin function approach is still capable to recreate the measured magnetization curves with comparatively good accuracy. The general influence on the slope that can be observed at different mechanical loads, is followed by the simulation results. The maximum values at the turning points of the different loaded curves as depicted in Fig.4 are met with high accuracy.

Despite of the acceptable general replication of the magnetization behavior for high excitations, the deviation between measured and simulated curves increases at higher mechanical stress levels. The error between measurements and simulations increases in the region of higher slope changes around the inflection point. The resulting simulated losses that were calculated by integrations over the simulated hysteresis loops, show and almost identical behavior with respect to the applied mechanical stress as the measured losses. But they remain constantly below the measured losses with offsets around $10\,\mathrm{W/m^3}$. This deviations between model and measurements

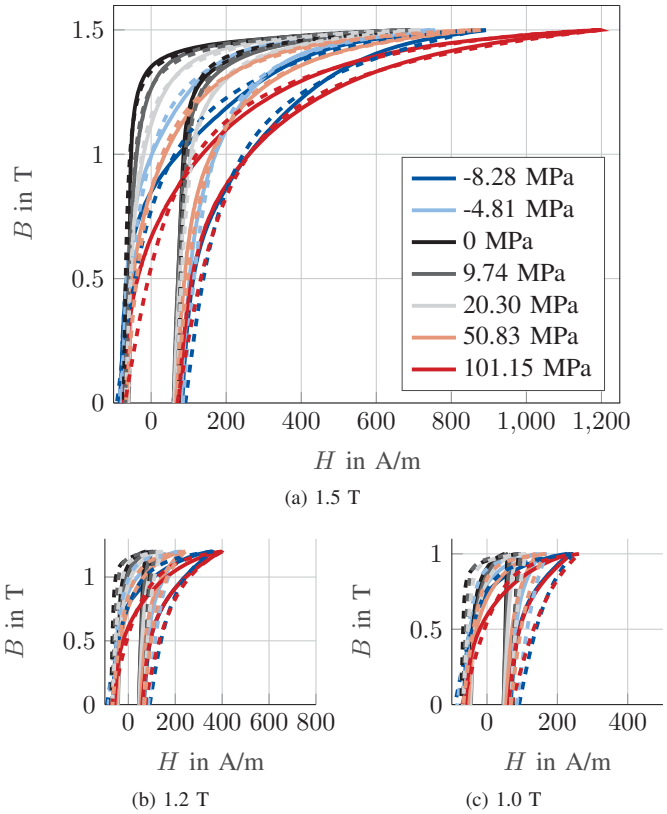

(a) 1.5 T

(b) 1.2 T

(c) 1.0 T

Fig. 3: Measured (solid) and simulated (dashed) hysteresis curves for different mechanic stresses.

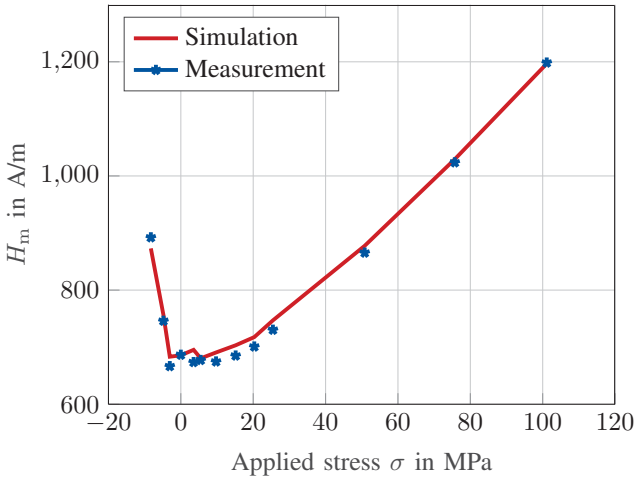

Fig. 4: Simulated and measured required maximum field H_m for saturations of 1.5 T with respect to the mechanical stress.

regarding the resulting losses and the flux paths around higher slope changes suggest a more detailed examination of the hysteretic magnetic field parts H_H, as they determine the width of the hysteresis and by this means the resulting simulated losses. A comparison between the measured and simulated width of the hysteresis curves is depicted in Fig. 6. At each mechanical load the deviation between measurement and simulation is remarkable. While the measurements reveal a variety of pathways with different characteristics for the respective stress levels, the simulations are bound to a uniform pathway by the Langevin function that is set in use during the basis equation of the hysteretic components (7). The deviations, that occur by this insufficiency of the the representation on H_H, interact again with the respective anhysteretic representations which have to compensate the misalignment between model an measurement.

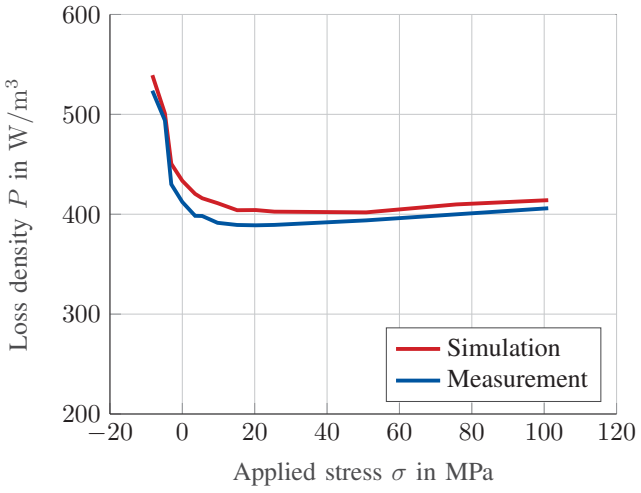

Fig. 5: Simulated and measured total hysteresis loss at 1.5 T for different mechanical stresses.

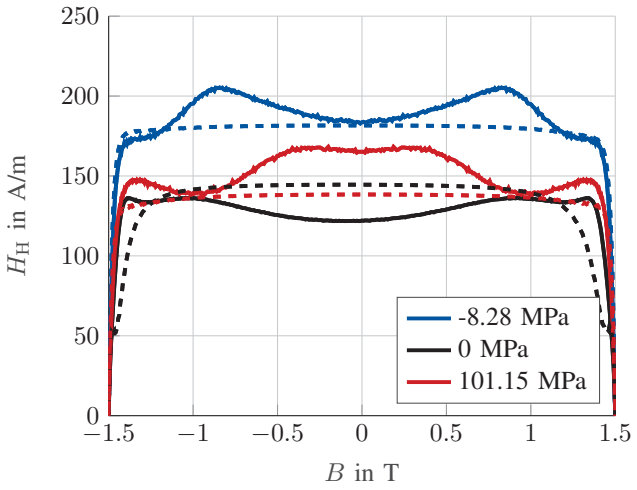

Fig. 6: Difference between measured (solid) and simulated (dashed) width of hysteresis determined by the hysteretic component H_{H}.

IV. Conclusion

In this paper the influence of mechanical stress on the magnetic properties is analyzed in terms of magnetization and loss behavior and modelled by an modified energy-based hysteresis model that is suitable for the use in finite-element machine simulations. The modified description of the anhysteretic magnetic field component leads to satisfactory accordance between measured behavior and their respective simulation results at different stress levels. The formulation of the hysteretic field component and the resulting hysteretic pathways were evaluated and compared to the actual measured pathways, revealing a lack of flexibility in the ground based set of equations. Further adjustments on the hysteresis model, particularly the description of the hysteretic field components particularly for decreasing excitations, as on the parameter identification routine could lead to clearer relationships between model parameters and applied mechanic stress and have to be investigated in subsequent studies. By this means the material behavior could be predicted continuously across the entire range of applied stress, by interpolating the identified parameter curves with respect to the mechanical load.

Acknowledgment

The work of the authors is performed in the research project group project "SP-2013 - The utilization of residual stresses induced by metal forming" funded by the Deutsche Forschungsgesellschaft (DFG) HA 4395/22-1 as DFG 255713208 and carried out in the research group project FOR 1897 Low-Loss Electrical Steel for Energy-Efficient Electrical Drives.

References

[1] Schneider, Carl S. "Effect of stress on the shape of ferromagnetic hysteresis loops." *Journal of applied physics* 97.10 (2005): 10E503.

[2] Leuning, N., Steentjes, S., Hameyer, K., Schulte, M., and Bleck, W. "Effect of Material Processing and Imposed Mechanical Stress on the Magnetic, Mechanical, and Microstructural Properties of HighSilicon Electrical Steel." *steel research international* 87.12 (2016): 1638-1647.

[3] Weiss, H. A., Leuning, N., Steentjes, S., Hameyer, K., Andorfer, T., Jenner, S., and Volk, W. "Influence of shear cutting parameters on the electromagnetic properties of non-oriented electrical steel sheets." *Journal of Magnetism and Magnetic Materials* 421 (2017): 250-259.

[4] Maurel, Vincent, Florence Ossart, and Ren Billardon. "Residual stresses in punched laminations: Phenomenological analysis and influence on the magnetic behavior of electrical steels." *Journal of Applied Physics* 93.10 (2003): 7106-7108.

[5] Yamazaki, Katsumi, and Yusuke Kato. "Iron loss analysis of interior permanent magnet synchronous motors by considering mechanical stress and deformation of stators and rotors." IEEE Transactions on Magnetics 50.2 (2014): 909-912.

[6] Ali, K., K. Atallah, and D. Howe. "Prediction of mechanical stress effects on the iron loss in electrical machines." Journal of applied physics 81.8 (1997): 4119-4121.

[7] Singh, D., Rasilo, P., Martin, F., Belahcen, A., and Arkkio, A. (2015). Effect of mechanical stress on excess loss of electrical steel sheets. IEEE Transactions on Magnetics, 51(11), 1-4.

[8] Karthaus, J., Steentjes, S., Leuning, N., and Hameyer, K. (2017). Effect of mechanical stress on different iron loss components up to high frequencies and magnetic flux densities. COMPEL-The international journal for computation and mathematics in electrical and electronic engineering, 36(3), 580-592.

[9] Bernard, Laurent, and Laurent Daniel. "Effect of stress on magnetic hysteresis losses in a switched reluctance motor: Application to stator and rotor shrink fitting." IEEE Transactions on Magnetics 51.9 (2015): 1-13.

[10] Rasilo, P., Steentjes, S., Belahcen, A., Kouhia, R., and Hameyer, K. "Model for Stress-Dependent Hysteresis in Electrical Steel Sheets Including Orthotropic Anisotropy." IEEE Transactions on Magnetics, 2017, 53. Jg., Nr. 6, S. 1-4.

[11] Sadowski, N., Batistela, N. J., Bastos, J. P. A., and Lajoie-Mazenc, M. "An inverse Jiles-Atherton model to take into account hysteresis in time-stepping finite-element calculations." IEEE Transactions on Magnetics 38.2 (2002): 797-800.

[12] Koltermann, P. I., Righi, L. A., Bastos, J. P. A., Carlson, R., Sadowski, N., and Batistela, N. J. "A modified Jiles method for hysteresis computation including minor loops." Physica B: Condensed Matter 275.1-3 (2000): 233-237.

[13] Bertotti, Giorgio. Hysteresis in magnetism: for physicists, materials scientists, and engineers. Academic press, 1998.

[14] Steentjes, S., Petrun, M., Glehn, G., Dolinar, D., and Hameyer, K. "Suitability of the double Langevin function for description of anhysteretic magnetization curves in NO and GO electrical steel grades." AIP Advances 7.5 (2017): 056013.

[15] Jiles, D. C., and Atherton, D. L. (1986). Theory of ferromagnetic hysteresis. Journal of magnetism and magnetic materials, 61(1-2), 48-60.

[16] Steentjes, S., Chwastek, K., Petrun, M., Dolinar, D., and Hameyer, K. (2014). Sensitivity analysis and modeling of symmetric minor hysteresis loops using the GRUCAD description. IEEE Transactions on Magnetics, 50(11), 1-4.